Micromagnetic simulation of the ground states of Ce-Fe-B amorphous nanodisks

D. Liu, G. Li, X. Zhao, J. F. Xiong, R. Li, T. Y. Zhao, F. X. Hu, J. R. Sun, and B. G. Shen

Citation: AIP Advances **8**, 056011 (2018); doi: 10.1063/1.5006447
View online: https://doi.org/10.1063/1.5006447
View Table of Contents: http://aip.scitation.org/toc/adv/8/5
Published by the American Institute of Physics

Micromagnetic simulation of the ground states of Ce-Fe-B amorphous nanodisks

D. Liu,[1,2] G. Li,[1,2] X. Zhao,[1,2] J. F. Xiong,[1,2] R. Li,[1,2] T. Y. Zhao,[1,2] F. X. Hu,[1,2] J. R. Sun,[1,2] and B. G. Shen[1,2,a]
[1]*State Key Laboratory of Magnetism, Institute of Physics, Chinese Academy of Sciences, Beijing 100190, P. R. China*
[2]*University of Chinese Academy of Sciences, Beijing 100049, P. R. China*

(Presented 10 November 2017; received 25 September 2017; accepted 23 October 2017; published online 15 December 2017)

Using 3D micromagnetics package OOMMF, the ground states of $Ce_2Fe_{14}B$ amorphous nanodisks with different dimensions, initial magnetization states and magnetocrystalline anisotropy constants (K) in zero external field were investigated. The simulations indicate that the disk size is the decisive factor in determining magnetic configurations. A diagram is constructed to bring out the dependence of the different equilibrium states on the disk thickness and diameter. When the ratio of thickness (T) to diameter (D) is smaller than 1, the vortex state is energetically more favorable than other states and the eigenfrequency of vortex approximately proportional to $(T/D)^{1/2}$. A variety of magnetization distributions of ground states for different anisotropy strengths is obtained. The result shows the magnetocrystalline anisotropy not only shrinks or broadens the vortex core but also induces an out-of-plane magnetization component both at the edge and the center of disks. When the K strength reaches a threshold value, there is a transition from vortex state to Bloch-type Skyrmion state which suggests the possibility of Skyrmion in rare-earth materials. In addition, in the system with specific aspect ratio and low intrinsic anisotropy, the vortex domain can always be sustained under various initial conditions. Meanwhile, the existence of stable vortex domain is found by experimentation in amorphous Ce-Fe-B ribbons which is in good agreement with the simulation result.
https://doi.org/10.1063/1.5006447

I. INTRODUCTION

RE-Fe-B (*RE* = rare earth) permanent magnets are widely used because of their excellent magnetic performance at room temperature.[1] However, due to the high price and short supply of *RE* metals, especially for Nd, Dy and Pr, many researchers have attempted to develop alternative and economically more attractive permanent magnets. Among all the rare earth elements, cerium (Ce) is the most abundant metallic element and its price is less than one-tenth of neodymium. Therefore, the alloys related to Ce have been employed to prepare more economic magnetic materials.[1,2] However, most of the investigations focused on Ce-Fe-B crystal alloys, the behavior of amorphous alloys was seldom referred.

In this paper, magnetic ground states of Ce-Fe-B amorphous alloys were studied not only for the basic investigation but also for their potential technological applications such as magnetic storage, random access memory devices and medical applications.[3] In order to have a measurable study on the effect of dimensions, initial magnetization states and magnetocrystalline anisotropy constants on the magnetic ground state before the further experimental study, a micromagnetic simulation on a magnetic microdisk was performed. To solve for the ground state, the Landau–Lifschitz–Gilbert

[a]Corresponding author: shenbaogen@yeah.net

(LLG) dynamic equation as a function of time was used to find the magnetization which will produce the lowest total energy. By studying the magnetic domain structure of Ce-Fe-B amorphous materials, the new understandings gained could lead to new potential applications except for low-cost permanent magnets.

II. SIMULATION METHOD

The Numerical method is widely used as a tool to describe the dynamics of magnetization in ferromagnetic materials.[4] The total Gibbs free energy (E_{tot}) consists of Zeeman energy (E_{ext}), magnetocrystalline anisotropy energy (E_{ani}), exchange energy (E_{exc}) and demagnetization energy (E_d):

$$E_{tot} = E_{ext} + E_{ani} + E_{exc} + E_d. \tag{1}$$

The ground magnetization configuration of the material is obtained by the LLG dynamic equation as a function of time:[5,6]

$$\frac{d\mathbf{M}}{dt} = -\gamma \mathbf{M} \times \mathbf{H_{eff}} + \frac{\alpha}{M}\mathbf{M} \times \frac{d\mathbf{M}}{dt}, \tag{2}$$

where $\mathbf{M}$ is the magnetization, $\mathbf{H_{eff}}$ is the effective field, γ is the Landau–Lifshitz gyromagnetic ratio and α is the dimensionless damping coefficient. The effective field is the functional derivative of the energy density which is defined as follows:

$$\mathbf{H_{eff}} = \frac{2A}{\mu_0 M_s^2}\nabla^2 \mathbf{M} - \mathbf{H_d} + \frac{2K_1}{\mu_0 M_s^2}(\mathbf{M} \cdot \hat{u})\,\hat{u}, \tag{3}$$

where $\hat{u}$ is the unit vector along the anisotropy axis and $\mathbf{H_d}$ is the demagnetizing field.

Micromagnetic simulations were performed using the 3D micromagnetic package OOMMF[7] and the simulation model was set to be a magnetic nanodisk. The material parameters for $Ce_2Fe_{14}B$ amorphous alloys used in the calculation at room temperature are as follow:[8] the saturation magnetization Ms = 9.3×10^5 A/m and the exchange integral constant A = 5 PJ/m. The sample was discretized into cell sizes of $2.5\times2.5\times2.5$ nm^3, ensuring that for each mesh the average edge length of all the tetrahedral elements was less than the exchange length of $Ce_2Fe_{14}B$ $L_{ex} = \sqrt{2A/\left(\mu_0 M_s^2\right)} = 3$ nm. Considering the simulating time and the precision, gyromagnetic ratio $\gamma = 2.211\times10^5$ mA^{-1}s^{-1} and damping coefficient $\alpha = 0.05$ were chosen. The thickness, diameter and magnetocrystalline anisotropy constant of each model will be given in response to the different situations below.

III. RESULTS AND DISCUSSION

By altering diameter (D) and thickness (T), the effects of different model dimensions on the equilibrium state are examined which are shown in FIG. 1. The initial state in this study is set to be a thermally neutralized state without any intrinsic anisotropy or external field. As such, the calculated magnetic configuration is simply the result of the competition between the demagnetizing field and exchange energy. The former favors a closed flux arrangement which necessitates a highly non-uniform spin arrangement due to the sample geometry while the latter favors uniform magnetization which inevitably generates magnetic poles at the sample surface. Depending on the disk diameter and thickness, metastable magnetic configurations are observed including the onion, vortex, and other different magnetic states. The largest disk diameter in this study is 250 nm while the smallest is 5 nm, with different thickness-to-diameter ratio T/D ranging from 1/5 to 10/1. Specifically, when the T/D is much smaller than 1, the vortex state is energetically more favorable than other states. While in some thicker disks, a much more pronounced magnetization canting can be seen, because when the disk thickness becomes much smaller than the diameter, the magnetization essentially aligns with the disk geometry so as not to lose too much exchange energy, but to cancel the total dipole energy. Due to the directions of magnetic moment remain confined in-plane, the angle between adjacent moments of the disk center becomes increasingly larger. Therefore, the magnetization at the core of the vortex structure will become perpendicular to the plane.

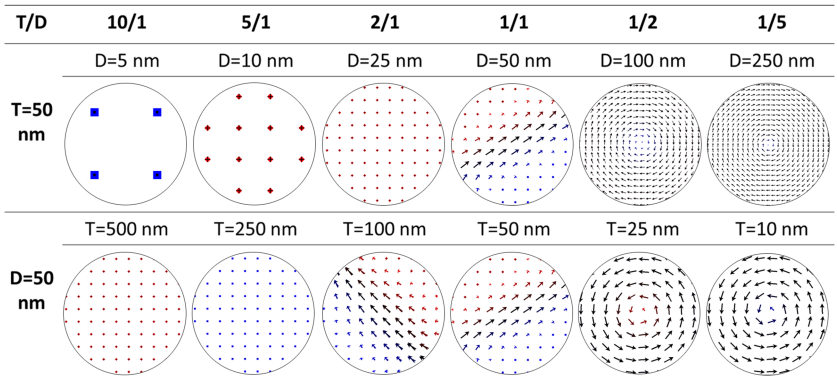

FIG. 1. The dependence of magnetization configuration of the equilibrium state on its geometrical parameters. The arrows are the projection of the in-plane magnetization where the red and blue represent the direction of +z and –z, respectively.

The numerical simulation shows that the size of model has a great effect not only on the steady state but also on the frequency response which is essentially useful for its potential applications in high-density magnetic storage and spin electronic devices. The temporal evolution of the average normalized magnetization component in x-direction (mx) is investigated by dynamic micromagnetic simulation. It can represent that the vortex core moves in y-direction.[9,10] And the corresponding resonance frequency ω is obtained by Fourier transformation of the time-domain oscillation.[11] The variation of the nanodisks resonance frequencies as a function of the ratio T/D is illustrated in FIG. 2 (the black square curve). The resonance frequency decreases abruptly as the disk ratio decreases from 10/1 to 1/1. When the aspect ratio T/D = 1, the resonance frequency drops to a minimum value of 0.43GHz. When the aspect ratio T/D ≤ 1/2, the resonance frequency decreases gradually with the ratio reducing. The resonance frequency originates from the confinement of the vortex core. A similar result was reported by Guslienko,[12] the eigenfrequency of magnetic disk depends on the aspect ratio T/D, approximately proportional to $(T/D)^{1/2}$ if the aspect ratio is much less than 1.

With a fixed model size in which the ratio of T/D is much less than 1 (T = 20 nm, D = 100 nm), the influence of initial state on magnetization configuration of equilibrium state is investigated. Starting with the magnetization in the random state, vortex state, x-direction, and z-direction, the model relaxes in no external field or anisotropy, solving for their corresponding ground states. As one can see in FIG. 3, the magnetization configuration of each system exhibits the vortex magnetization distribution with different chirality. The positions of vortex center for four different initial states

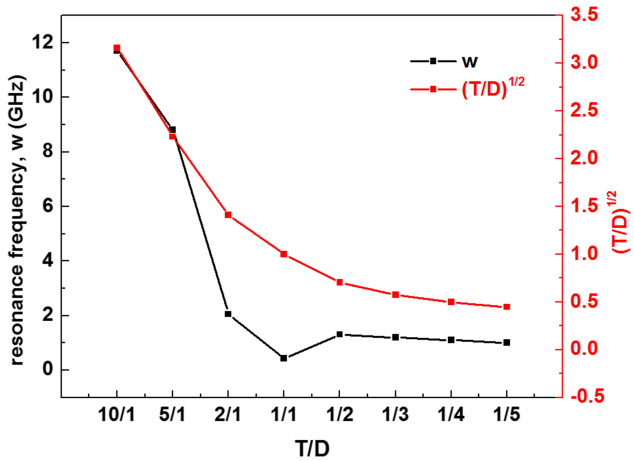

FIG. 2. The spectra for resonance frequency of amorphous disks with different aspect ratios. The black squares are points simulated numerically, the red line corresponds to fitting using the equation $\omega \sim (T/D)^{1/2}$.

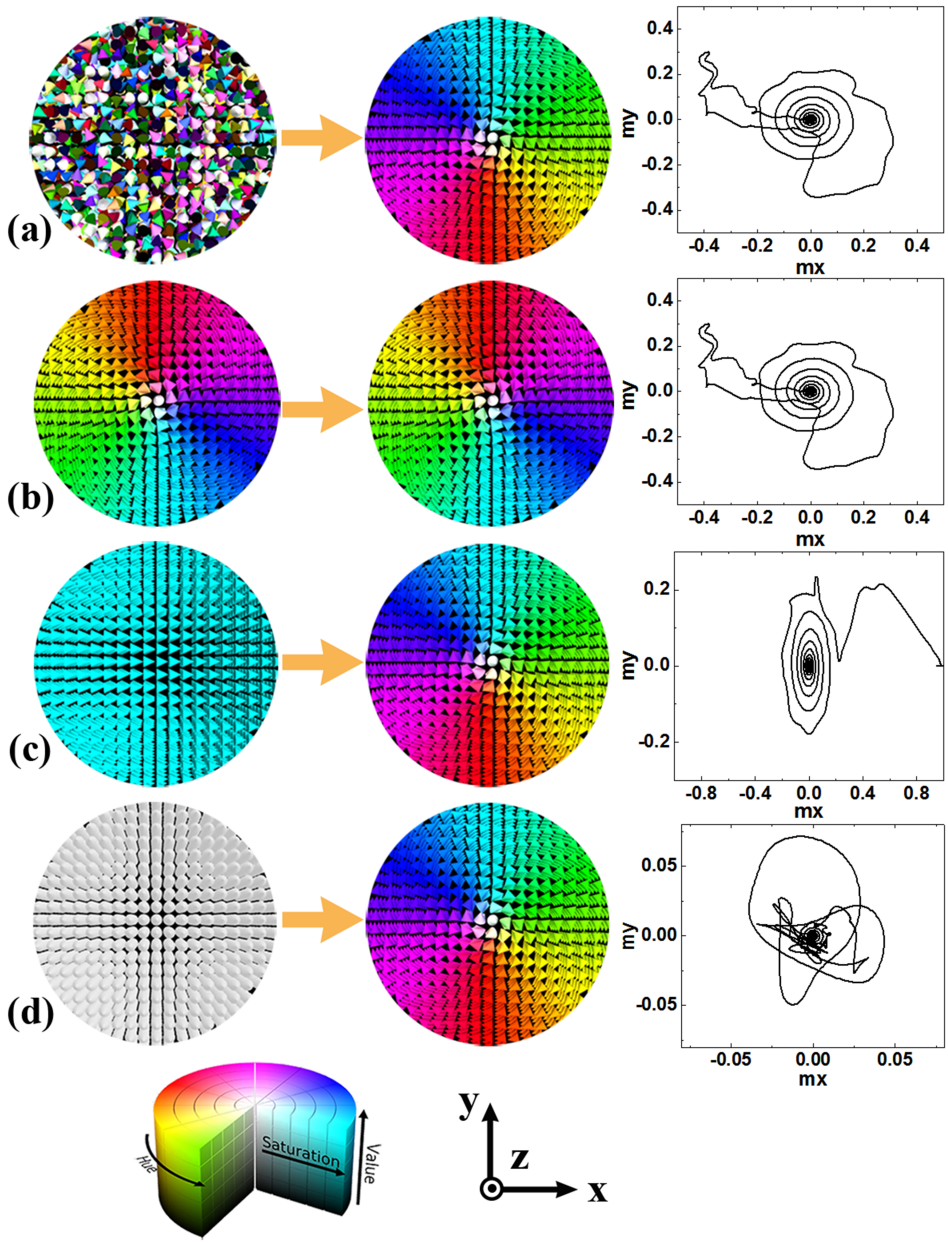

FIG. 3. Magnetic configuration and the movements of vortex center for four different initial states: (a) thermal demagnetization state, (b) vortex state, (c) in the x-direction and (d) in the z-direction on the left side and corresponding equilibrium states of each system on the right side. The HSL color scale reflects the variation of a component of the magnetization in full orientation.

stable in the same place when the systems achieve their stability. In addition, each energy item of each system becomes the same, which is $E_{tot} = 2.88\times10^{-18}$ J, $E_{ani} = 7.28\times10^{-19}$ J and $E_{exc} = 2.15\times10^{-18}$ J, respectively. As one can conclude in this situation, the ground state of this system with low anisotropy is a vortex magnetization distribution, unconnected to the initial magnetization. The existence of magnetic vortex is found by experimentation investigations in amorphous $Ce_{14}Fe_{80}B_6$ ribbons which consonant with the simulation result.[13]

Compared to other parameters of magnetic materials, the degree of amorphization affected magnetocrystalline anisotropy (K) most. To clarify the role of the anisotropy contribution, the stable magnetic configuration for K = 0 J/m^3 is simulated first, and then by gradually varying the K value how the anisotropy influences the magnetic configuration is studied. Applying the

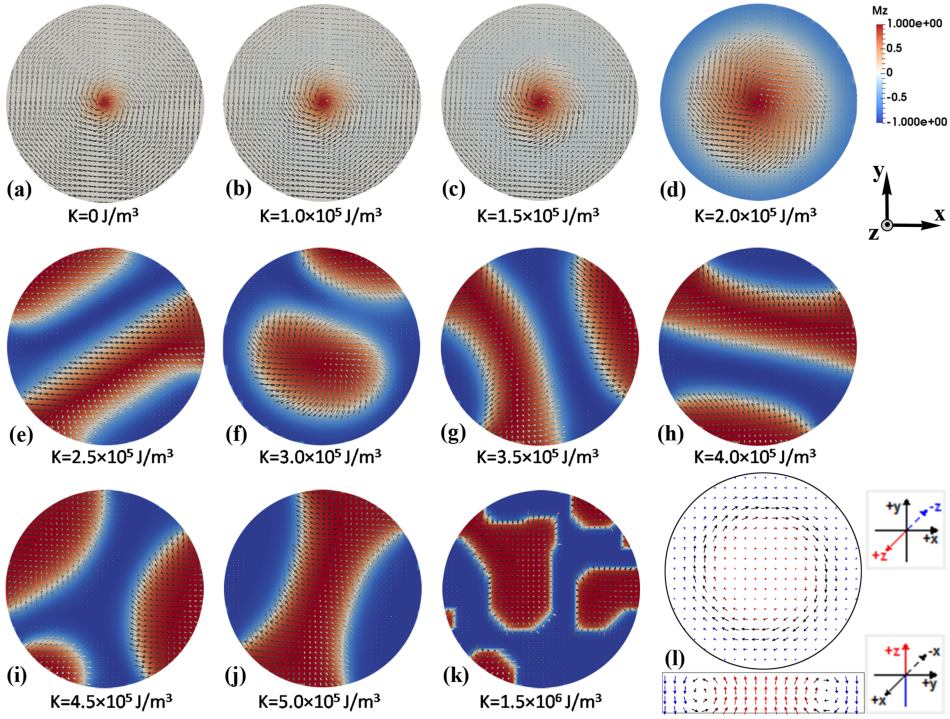

FIG. 4. (a) - (k) Schematic representation of equilibrium states that form at H = 0 investigated under different values of K for D =100 nm and T=20 nm. (l) The Bloch-type Skyrmion observed at K = 2.8×10^5 J/m^3. Mz is the z components of magnetization and represented by regions in red (+z) and blue (-z).

same procedure of the energy minimization, the ground states diagram is obtained and presented in FIG. 4. The initial distribution of the magnetic moments is random and the easy axis of the anisotropy is +z.

From FIG. 4(a) to FIG. 4(d), the ground state of the system with low anisotropy keeps a vortex magnetization distribution. Coincide with previous results, vortex state is a typical situation for soft magnetic materials in symmetric structure taken exchange and magnetostatic interactions into account only.[14,15] For K < 2.5×10^5 J/m^3, the size of the vortex core will increase with the increasing K until the vortex state breaks into another phase for the strong anisotropy. The effect of changing anisotropy and Dzyaloshinskii-Moriya (DM) interaction have a similar impact on the vortex in magnetic nanodisk.[16] The magnetocrystalline anisotropy induces an out-of-plane magnetization component both at the edge and the center of disks. There is a phase transition from the vortex state to the Bloch-type Skyrmion when the K strength reaches a threshold value. The threshold value which depends on the disk parameters in this simulation is 2.8×10^5 J/m^3 (FIG. 4(l)). This simulation result indicates that the Skyrmion state will appear spontaneously in the rare-earth amorphous material which agrees well with theoretical prediction.[17] Spontaneous Skyrmion lattice ground states may exist generally in condensed matter systems having chiral interactions without the assistance of external fields or defects. Coincidentally, Montoya et al.[18] found that the stabilization of Skyrmions in amorphous Fe/Gd is purely driven by tuning magnetic properties and film thickness and that no DMI is present in these films. The results provide a guideline for engineering the formation and controllability of Skyrmion phases in symmetrical structure. Moreover, as the value of K continues to increase, the influence of K leads to an asymmetric deformation of the Bloch-type Skyrmion such that the magnetization is orientated generally along the normal vector z.

IV. CONCLUSION

In conclusion, using the numerical micromagnetic model, magnetization ground states of Ce-Fe-B amorphous disks for different aspect ratios T/D, initial magnetizations and magnetocrystalline

anisotropy constants are systematically investigated. The simulations show that the vortex state can appear as a steady state for specific range of T/D which is significantly smaller than 1. In addition, the system with low anisotropy favors the formation of vortex configuration under various initial magnetization state, which will contribute to other applications except for hard magnets. A variety of magnetization distributions of ground states for various anisotropy strengths is obtained. The results indicate that the existence of the magnetocrystalline anisotropy not only shrinks or broadens the vortex core but also induces an out-of-plane magnetization component both at the edge and the center of disks, which cause the generation of Skyrmion. Therefore, fabricating RE-Fe-B magnets by using Ce is highly beneficial to utilize the rare-earth resource in a balanced manner and manufacture low-cost magnets.

ACKNOWLEDGMENTS

This work was supported by the National Key Research Program of China (Grant No. 2014CB643702, Grant No. 2016YFB0700903), the National Natural Science Foundation of China (Grant No. 51590880) and the Knowledge Innovation Project of the Chinese Academy of Sciences (Grant No. KJZD-EW-M05).

[1] E. Burzo, Rep. Prog. Phys. **61**, 1099 (1998).
[2] J. F. Herbst, M. S. Meyer, and F. E. Pinkerton, J. Appl. Phys. **111**, 07A718 (2012).
[3] M. E. Mchenry, M. A. Willard, and D. E. Laughlin, Prog. Mater Sci. **44**, 291 (1999).
[4] J. G. Zhu, Y. Zheng, and G. A. Prinz, J. Appl. Phys. **87**, 6668 (2000).
[5] L. D. Landau and E. M. Lifshitz, Phys. Z. Sowjetunion **8**, 153 (1935).
[6] T. L. Gilbert, Phys. Rev. **100**, 1243 (1955).
[7] M. J. Donahue and D. G. Porter, OOMMF User's Guide, version 1.0, Interagency Report NISTIR 6376, National Institute of Standards and Technology, Gaithersburg, MD, (1999).
[8] J. F. Herbst, Rev. Mod. Phys. **63**, 819 (1991).
[9] K. Yu. Guslienko, B. A. Ivanov, V. Novosad, Y. Otani, H. Shima, and K. Fukamichi, J. Appl. Phys. **91**, 8037 (2002).
[10] K. X. Xie, W. W. Lin, P. Zhang, and H. Sang, Appl. Phys. Lett. **105**, 102402 (2014).
[11] V. Novosad, M. Grimsditch, K. Yu. Guslienko, P. Vavassori, Y. Otani, and S. D. Bader, Phys. Rev. B **66**, 052407 (2002).
[12] K. Y. Guslienko, W. Scholz, R. W. Chantrell, and V. Novosad, Phys. Rev. B: Condens. Matter **71**, 4407 (2004).
[13] S. L. Zuo, M. Zhang, R. Li, Y. Zhang, L. C. Peng, J. f. Xiong, D. Liu, T. Y. Zhao, F. X. Hu, B. G. Shen, and J. R. Sun, Acta Mater. **140**, 465 (2017).
[14] R. P. Cowburn, D. K. Koltsov, A. O. Adeyeye, M. E. Welland, and D. M. Tricker, Phys. Rev. Lett. **83**, 1042 (1999).
[15] V. P. Kravchuk, D. D. Sheka, and Y. B. Gaididei, J. Magn. Magn. Mater. **310**, 116 (2007).
[16] Y. M. Luo, C. Zhou, C. Won, and Y. Z. Wu, AIP Advances **4**, 047136 (2014).
[17] U. K. Rössler, A. N. Bogdanov, and C. Pfleiderer, Nature **442**, 797 (2006).
[18] S. A. Montoya, S. Couture, J. J. Chess, J. C. T. Lee, N. Kent, D. Henze, S. K. Sinha, M. Y. Im, S. D. Kevan, P. Fischer, B. J. McMorran, V. Lomakin, S. Roy, and E. E. Fullerton, Phys. Rev. B **95**, 024415 (2017).